

Anomaly in Nonlinear Magnetoelectric Response of YbMnO₃

U. Adem,¹ M. Mostovoy,¹ N. Bellido,² A. A. Nugroho,^{1,3} C. Simon,² and T. T. M. Palstra¹

¹*Zernike Institute for Advanced Materials, University of Groningen, 9747 AG Groningen, The Netherlands*

²*Laboratoire CRISMAT, UMR CNRS ENSICAEN, 1450 Caen, France*

³*Faculty of Mathematics and Natural Sciences, Institut Teknologi Bandung, Jl. Ganesha 10, Bandung 40132, Indonesia*

(Dated: November 6, 2018)

We observe a seemingly complex magnetic field dependence of dielectric constant of hexagonal YbMnO₃ near the spin ordering temperature. After rescaling, the data taken at different temperatures and magnetic fields collapse on a single curve describing the sharp anomaly in nonlinear magnetoelectric response at the magnetic transition. We show that this anomaly is a result of the competition between two magnetic phases. The scaling and the shape of the anomaly are explained using the phenomenological Landau description of the competing phases in hexagonal manganites.

PACS numbers: 77.80.-e, 61.10.Nz, 77.84.-s

The recent interest in multiferroic materials was triggered by the discovery of the giant magnetocapacitance (MC) and magnetically-induced rotations of electric polarization in orthorhombic rare earth manganites [1, 2, 3]. This multiferroic behavior is rooted in magnetic frustration, which gives rise to non-centrosymmetric spin orderings that induce electric polarization [4]. Furthermore, the presence of competing spin states in these frustrated magnets results in a strong sensitivity of the magnetically-induced electric polarization to applied magnetic fields. In this respect multiferroics are similar to colossal magnetoresistance manganites and high-temperature superconductors [5].

In this Letter we study effects of critical magnetic fluctuations and the competition between different magnetic states on the non-linear magnetoelectric response of the hexagonal YbMnO₃ by measuring the magnetic field and temperature dependence of its dielectric constant. Ferroelectricity in hexagonal manganites $R\text{MnO}_3$ ($R = \text{Ho-Lu, Y}$) appears well above the magnetic transition and is of nonmagnetic origin: An electric dipole moment along the c axis is spontaneously induced by tilts of manganese-oxygen bipyramids and buckling of rare earth-oxygen planes at $T_C > 600\text{K}$ [6, 7, 8, 9], while the ordering of Mn spins occurs at a much lower temperature $T_N < 120\text{K}$. However, the spin ordering in hexagonal manganites results in a surprisingly strong lattice relaxation, which affects the spontaneous electric polarization [10].

The Mn ions in hexagonal manganites form well-separated triangular layers parallel to the ab plane with antiferromagnetic exchange interactions between nearest-neighbor spins [11], which makes the Mn spin subsystem low-dimensional and frustrated and results in enhanced spin fluctuations observed well above T_N [12]. Frustration and rare earth magnetism are responsible for a rich variety of magnetic phases observed at low temperatures and in applied magnetic fields [13]. Due to magnetoelectric coupling each magnetic transition gives rise to a singularity of the dielectric constant [6, 14, 15, 16], which is more pronounced than the corresponding singularity in

magnetic susceptibility.

We find that close to the Néel temperature $T_N=81\text{K}$ the MC of YbMnO₃ measured as a function of magnetic field and temperature obeys a scaling behavior and has a very sharp anomaly. The detailed comparison with results of model calculations led us to a conclusion that the effect of magnetic fluctuations is completely overshadowed by the magnetic field dependence originating from the competition between two antiferromagnetic states, one of which is weakly ferromagnetic. Using a mean field Landau expansion of free energy in powers of two competing order parameters, we reproduce the shape of the anomaly as well as the changes in the behavior of MC observed in the wide range of magnetic fields and temperatures.

Polycrystalline samples of YbMnO₃ were prepared by solid state synthesis. A single crystal was grown from this powder by the floating zone technique. Magnetization $M(T)$ of the samples was measured by a Squid magnetometer (MPMS7 Quantum Design) using a field of 0.5T. Field dependence of the magnetization was measured up to 5T. Capacitance of the samples was measured in a commercial system (PPMS Quantum Design) using a home-made insert and a Andeen-Hagerling 2500A capacitance bridge operating at a fixed measurement frequency of 1 kHz as well as using an Agilent 4284A LCR meter up to 1MHz. Electrical contacts were made using Ag epoxy.

The temperature dependence of the capacitance $C(T)$ proportional to the in-plane dielectric constant ε_a is shown as an inset of Fig. 1a. Below the Néel temperature $T_N = 82\text{K}$, the capacitance is somewhat suppressed by the emergence of magnetic order [16]. The MC, $\frac{C(H)-C(0)}{C(0)}$, where H is magnetic field along the c axis, for a set of temperatures between 76.5K and 95K is shown in Fig. 1a. In this small temperature interval around T_N the behavior changes dramatically: at 76.5K only a positive curvature is observed. With increasing temperature a high-field downturn appears, and at 80K only a negative curvature can be observed, which changes

back to positive above 90K.

This unusual behavior is a consequence of the fact that by varying temperature and magnetic field we force the system to pass through a magnetic transition. The critical behavior becomes apparent when we plot $\frac{C(H)-C(0)}{C(0)H^2}$ vs temperature [see Fig. 1(b)]. The procedure to evaluate ΔC at fixed magnetic fields versus temperature i.e. replotting the rescaled changes of dielectric constant in magnetic field versus temperature, effectively reveals the magnetic field dependence of C . The strong temperature dependence of C masks the magnetic field dependence when $C(T)$ is measured at fixed magnetic fields. The data taken at various T and H remarkably fall onto a single curve with a very sharp anomaly at T_N where the temperature derivative of MC becomes large and positive while its magnitude shows an almost discontinuous jump from a positive to a negative value. The observed scaling behavior of MC can be understood in terms of the anomalous nonlinear magnetoelectric response, described by the term $\kappa(T) (E_a^2 + E_b^2) H_c^2$ in free energy, where $\kappa(T)$ has a singularity at the magnetic transition temperature. The scaling implies that the dependence of magnetic susceptibility for $H||c$ on electric field $E||a$ has the same anomaly at T_N .

The shape of the MC anomaly in YbMnO_3 is unusual. The nonlinear magnetoelectric response in antiferromagnets usually originates from the ubiquitous fourth-order coupling of the electric polarization P to the magnetic order parameter L , $f_{me} = \frac{g}{2} P^2 L^2$. It results in a correction to the bare dielectric susceptibility χ_0 , $\delta\chi = -g\chi_0^2 \langle L \rangle^2 \propto (-\tau)^{2\beta}$, for $\tau = \frac{T-T_N}{T_N} < 0$, which accounts for the observed dielectric constant anomaly below T_N [see the inset of Fig. 1(a)]. The magnetic field dependence of Néel temperature, $T_N(H) \approx T_N(0) - \lambda H^2$, gives rise to a discontinuity of MC at T_N and its anomalous behavior below T_N , is roughly consistent with our data. However, the most prominent feature of the observed anomaly – the long negative tail for $T > T_N$ [see Fig. 1(b)] – cannot be explained in this way.

This tail may result from magnetic fluctuations that become critical close to Néel temperature. The two lowest-order self-energy diagrams describing contributions of magnetic fluctuations to dielectric susceptibility are shown in Fig. 2. The lowest-order term is given by $\delta\chi^{(1)} = -g\chi_0^2 (\langle L^2 \rangle - \langle L \rangle^2) \propto \tau^{1-\alpha}$, where α is the exponent describing the critical behavior of magnetic specific heat [6, 17]. The corresponding singularity in MC $\propto g\lambda \text{sign}(\tau) |\tau|^{-\alpha}$ ($g, \lambda > 0$ for YbMnO_3), is positive for $T > T_N$, in disagreement with our data. The second-order fluctuational correction [see Fig. 2(b)], $\delta\chi^{(2)} = \frac{2(g\chi_0 P_0)^2}{k_B T} \int d^3x [\langle L^2(\mathbf{x}) L^2(0) \rangle - \langle L^2 \rangle^2]$, results in the MC anomaly $\propto -\lambda \text{sign}(\tau) |\tau|^{-1-\alpha}$, which has the shape similar to that observed experimentally. However, this term is only nonzero in a ferroelectric state with a

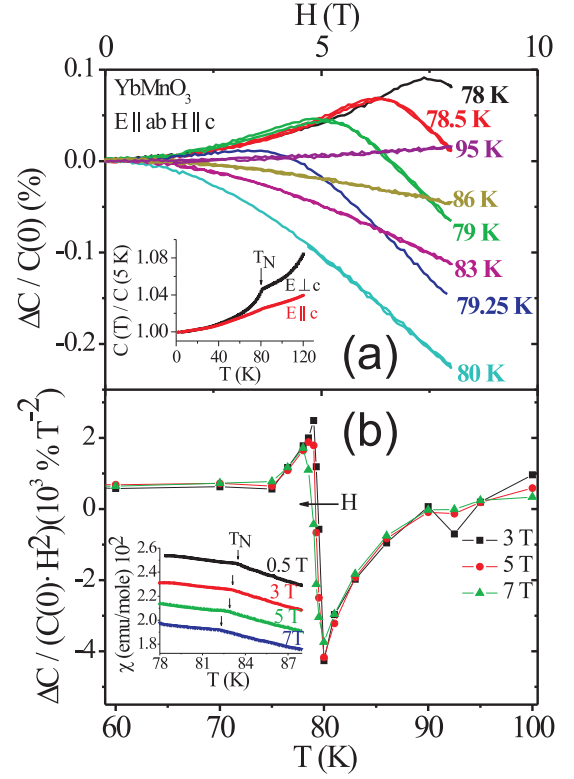


FIG. 1: (Color online) (a) Magnetic field dependence of MC of YbMnO_3 single crystal at constant temperatures near T_N . The temperature dependence of capacitance is added as an inset. (b) Temperature dependence of MC at constant magnetic fields. The inset shows the shift of T_N in magnetic field obtained from magnetic susceptibility measurements. Electric field is parallel to the ab plane, while $H||c$.

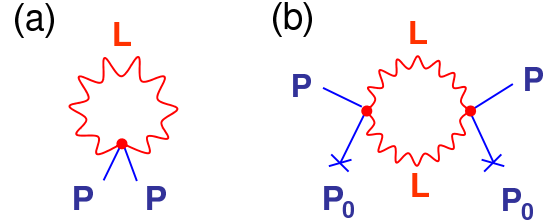


FIG. 2: (Color online) The self-energy diagrams of the first (a) and second (b) order in the coupling constant g , describing contributions of magnetic fluctuations (wavy lines) to dielectric susceptibility.

spontaneous polarization $P_0 \neq 0$ and, therefore, should be visible in ϵ_c , while we observe an anomaly only in $\epsilon_{a,b}$.

From this we conclude that the observed anomaly is unrelated to magnetic fluctuations and originates from a different physics. Below we show that the shape and scaling behavior of MC can be explained within a mean field theory by the competition between antiferromagnetic and weakly ferromagnetic state.

Hexagonal manganites show a number of magnetic phases with the 120° -angle between Mn spins in triangu-

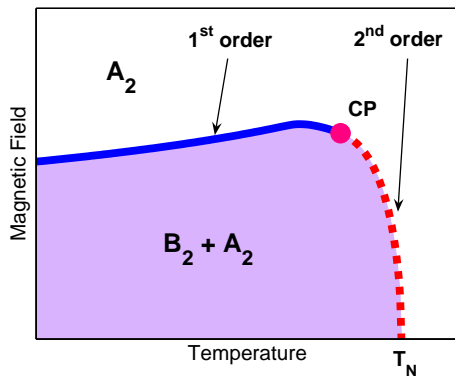


FIG. 3: (Color online) The magnetic phase diagram of the model Eq.(1) for $T_B^{(0)} > T_A^{(0)}$. The lilac region is the B_2 phase with some admixture of the A_2 phase. The critical point (CP) separates the first-order transition (solid) line from the second-order transition (dashed) line.

lar ab layers [18]. These phases differ by orientation of the spins with respect to the crystallographic axes and spins in neighboring layers as well as by the ordering of rare earth spins [19, 20, 21, 22]. The magnetic phase diagram of YbMnO_3 studied by a variety of different experimental techniques includes the low-field B_2 phase (magnetic space group $P6_3cm$) and the high-field A_2 -phase (magnetic space group $P6_3cm$) [18, 23]. The symmetry of the latter state allows for a net magnetization in the c direction (largely due to the rare earth spins and therefore small near the Mn spin-ordering temperature), which is why the A_2 phase is stabilized by $H\parallel c$.

The competition between the A_2 and B_2 phases was discussed in Ref. [24] using the phenomenological free energy expansion in two order parameters:

$$f = \sum_{\gamma=A,B} \left[\frac{\alpha_\gamma}{2} (T - T_\gamma^{(0)} + \lambda_\gamma H^2) L_\gamma^2 + \frac{b_\gamma}{4} L_\gamma^4 \right] + \frac{d}{2} L_A^2 L_B^2 - H \left(\phi L_A + \frac{\phi'}{3} L_A^3 + \frac{\phi''}{2} L_A L_B^2 \right) \quad (1)$$

where $L_A(L_B)$ is the order parameter describing the $A_2(B_2)$ phase and H is magnetic field along the c axis. The linear coupling of L_A to H corresponds to the spontaneous magnetization present in the A_2 phase.

The typical phase diagram for $T_B^{(0)} > T_A^{(0)}$ (when the B_2 phase is energetically more favorable than the A_2 phase at zero field) is shown in Fig. 3. Due to the linear coupling between H and L_A , the latter order parameter is nonzero for an arbitrarily weak magnetic field, so that for $H \neq 0$ the transition occurs between the A_2 phase and the B_2 phase with some admixture of the A_2 phase.

The MC for this model, shown in Fig. 4(c), is calculated by adding to the free energy Eq.(1) the terms describing the coupling of the magnetic order parameters

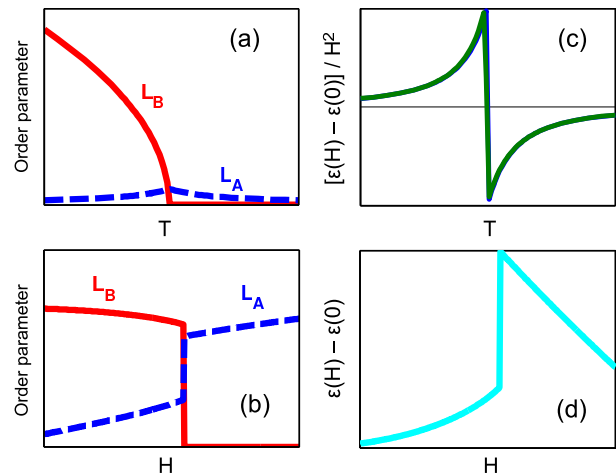


FIG. 4: (Color online) The temperature dependence of order parameters L_A (dashed blue line) and L_B (solid red line) near the second-order (a) and first-order (b) transitions. Panel (c) shows the anomaly in rescaled MC at the second-order transition temperature; the two curves calculated for different values of magnetic field are almost indistinguishable. The MC anomaly at the first-order transition is shown in panel (d).

to the in-plane electric polarization and the dielectric response of the nonmagnetic state,

$$\Delta f = \frac{P^2}{2} \left(\sum_{\gamma=A,B} g_\gamma L_\gamma^2 + g'_A L_A H \right) + \frac{P^2}{2\chi_0} - PE, \quad (2)$$

has the same shape as the one observed in YbMnO_3 and, for weak fields, obeys the observed scaling. This behavior can be understood by noting that the main contribution to the magnetic field dependence of the dielectric susceptibility comes from L_A , which is linearly coupled to H . This field-induced order parameter grows as T approaches the T_N from above [see Fig. 4(a)], which gives rise to the ‘high-temperature’ negative MC tail, as $\Delta\chi_e \propto -L_A^2$. In the weak-field regime $L_A \propto H$, so that $\frac{\chi_e(T,H) - \chi_e(T,0)}{H^2}$ is approximately field-independent, which explains the observed scaling [25].

As the magnetic field increases, the character of the transition in the two-parameter model changes: in low fields the transition is of second order (red dashed line in Fig. 3), while in high fields and low temperatures it becomes a first-order transition (blue line) [see also Figs. 4(a) and (b)]. The first- and second-order transition lines are separated by the critical point. This change in the nature of the transition is also clearly seen in the experiments by comparing the field-dependence of MC at low temperatures [see Fig. 5(a)] to that at high temperatures [see Fig. 1(a)]. At 2K the MC shows a distinct cusp at the first-order transition, which is well reproduced within our model [see Fig 4(d)]. In YbMnO_3 the changes in the order of the transition are made more dramatic by the fact that at low temperatures and high mag-

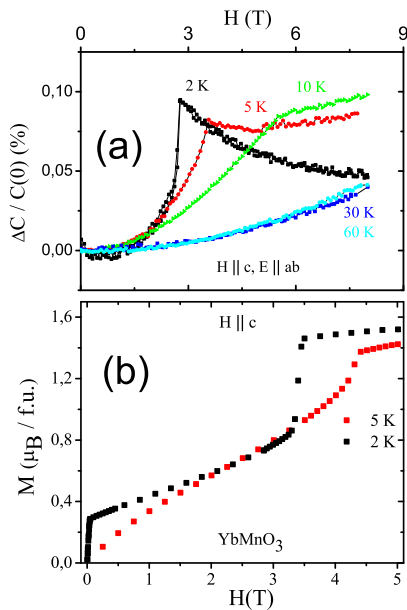


FIG. 5: (Color online) (a) MC of $YbMnO_3$ at $T < T_N$ for $E || ab$ -plane and $H || c$; (b) Field dependence of magnetization at 2 and 5 K.

netic fields magnetic response is dominated by Yb spins, which below 3.8 K order ferrimagnetically [23]. This leads to a strong decrease of the critical magnetic field at low temperatures ($H_c \sim 3$ T at 2 K) and gives rise to the sharp discontinuity in magnetization [see Fig. 5(b)] [26].

Finally, since the shape of the MC anomaly may be affected by the motion of antiferromagnetic domain walls separating different antiferromagnetic phases, we measured the frequency dependence of the dielectric constant. We found no frequency dependence in the interval from 1 kHz to 1 MHz, suggesting that the contribution of the domain walls in $YbMnO_3$ is negligible.

To summarize, we observed a sharp anomaly in nonlinear magnetoelectric susceptibility of the hexagonal rare earth manganite $YbMnO_3$ at the Néel temperature. We discussed theoretically possible sources of the anomaly and showed that it results from the competition between two antiferromagnetically ordered states of $YbMnO_3$, one of which has a small spontaneous magnetic moment. Even though this weakly ferromagnetic phase becomes the ground state only in rather high magnetic fields or at very low temperatures, its admixture to the non-ferromagnetic phase determines the shape of the MC anomaly along the whole critical line of magnetic phase transitions. The competition between different magnetic phases, some of which may have weak ferromagnetic moment is very common for frustrated magnets: similar phase diagrams were found for hexagonal $HoMnO_3$, which shows four competing states [18] and for $Ni_3V_2O_8$ [27]. Thus many other systems should show an anomaly in nonlinear magnetoelectric response, although its shape,

which depends on parameters of the Landau free energy, may vary from material to material.

We thank G.R. Blake, G.Nenért and N. Mufti for useful discussions and J. Baas for technical help. The work of A.A.N. is supported by the NWO Breedtestrategie Program of the Material Science Center, RuG and by KNAW, Dutch Royal Academy of Sciences, through the SPIN program. This work is in part supported by the Stichting FOM (Fundamental Research on Matter) and in part by the EU STREP program MaCoMuFi under contract FP6-2004-NMP-TI-4 STRP 033221.

-
- [1] T. Kimura, T. Goto, H. Shintani, K. Ishizaka, T. Arima, and Y. Tokura, *Nature (London)* **426**, 55 (2003).
 - [2] T. Goto, T. Kimura, G. Lawes, A.P. Ramirez, and Y. Tokura, *Phys. Rev. Lett.* **92**, 257201 (2004).
 - [3] N. Hur *et al.*, *Nature* **429**, 392 (2004).
 - [4] For a review, see S.-W. Cheong and M. Mostovoy, *Nature Materials* **6**, 13 (2007).
 - [5] See, e.g., J. Burgoyne, M. Mayr, V. Martin-Mayor, A. Moreo, and E. Dagotto, *Phys. Rev. Lett.* **87**, 277202 (2001) and references therein.
 - [6] T. Katsufuji *et al.*, *Phys. Rev. B* **64**, 104419 (2001).
 - [7] B. B. van Aken, T. T. M. Palstra, A. Filippetti, and N. A. Spaldin, *Nature Mater.* **3**, 164 (2004).
 - [8] C. J. Fennie and K. M. Rabe, *Phys. Rev. B* **72**, 100103(R) (2005).
 - [9] U. Adem, A. A. Nugroho, A. Meetsma, and T.T.M. Palstra, *Phys. Rev. B* **75**, 014108, (2007).
 - [10] S. Lee *et al.*, *Nature* **451**, 805 (2008).
 - [11] E. F. Bertaut *et al.*, *C.R. Acad. Sci. Paris* **256**, 1958, (1963).
 - [12] J. Park *et al.*, *Phys. Rev. B* **68**, 104426 (2003).
 - [13] B. Lorenz, A. P. Litvinchuk, M. M. Gospodinov, and C. W. Chu, *Phys. Rev. Lett.* **92**, 087204 (2004).
 - [14] Z. J. Huang, Y. Cao, Y. Y. Sun, Y. Y. Xue, and C. W. Chu, *Phys. Rev. B* **56**, 2623 (1997).
 - [15] H. Sugie, N. Iwata, and K. Kohn, *J. Phys. Soc. Jpn.* **71**, 1558 (2002).
 - [16] G. A. Smolenskii and I. E. Chupis, *Sov. Phys. Usp.* **25**, 475 (1982).
 - [17] G. Lawes, A.P. Ramirez, C.M. Varma, and M. A. Subramanian, *Phys. Rev. Lett.* **91**, 257208 (2003).
 - [18] M. Fiebig *et al.*, *J. Appl. Phys.* **93**, 8194 (2003).
 - [19] T. Lonkai *et al.*, *Appl. Phys. A* **74**, S843 (2002).
 - [20] A. Muñoz *et al.*, *Phys. Rev. B* **62**, 9498 (2000); *Chem. Mater.* **13**, 1497 (2001); *J. Phys. Condens. Matter* **14**, 3285 (2002).
 - [21] M. Fiebig *et al.*, *Phys. Rev. Lett.* **84**, 5620 (2000).
 - [22] M. Fiebig *et al.*, *J. Appl. Phys.* **91**, 8867 (2002).
 - [23] F. Yen, C. dela Cruz, B. Lorenz, E. Galstyan, Y. Y. Sun, M. Gospodinov, and C.W., Chu, *J. Mater. Res.*, **22**, 2163, (2007).
 - [24] I. Munawar and S. H. Curnoe, *J. Phys.: Condens. Matter* **18**, 9575 (2006).
 - [25] Another contribution to MC comes from an additional increase of L_B below T_N due to the suppression of L_A , which leads to the discontinuity and the sign change of MC at T_N . This contribution is also proportional to H^2 .

- [26] D. Tomuta, PhD Thesis, Leiden University, (2003).
- [27] G. Lawes *et al.*, Phys. Rev. Lett. **93**, 247201 (2004).